Mechanical behaviour of contractile gels based on light-driven molecular motors

Jean-Rémy Colard-Itté, Quan Li, Dominique Collin, Giacomo Mariani, Gad Fuks, Emilie Moulin, Eric Buhler, Nicolas Giuseppone

COMMUNICATION

Mechanical behaviour of contractile gels based on light-driven molecular motors

Received 00th January 20xx,
Accepted 00th January 20xx

DOI: 10.1039/x0xx00000x

Jean-Rémy Colard-Itté,[a] Quan Li,[a] Dominique Collin,[b] Giacomo Mariani,[c] Gad Fuks,[a] Emilie Moulin,[a] Eric Buhler,[c]* and Nicolas Giuseppone[a]*

The networking of individual artificial molecular motors into collective actuation systems is a promising approach for the design of active materials working out of thermodynamic equilibrium. Here, we report the first mechanical studies on active polymer gels built by integrating light-driven rotary molecular motors as reticulation units in polymer networks. We correlate the volume ratio before and after light irradiation with the change of elastic modulus, and we reveal a universal maximum mechanical efficiency of such gels related to their critical overlap concentration before chemical reticulation. We also show the major importance of heterogeneities in the macroscopic contraction process and we confirm that these materials can increase their internal energy by the motorized winding of their polymer chains.

Introduction

The harnessing of individual molecular machines into large integrated systems finds its most striking example in muscular tissues. From a simplified structural and thermodynamic point of view, muscles integrate biomolecular motors[1,2] (myosin heads) that produce collective out-of-equilibrium pulling motions within a network of biopolymers (actin and myosin filaments) when supplied with an external source of energy in the form of adenosine triphosphate (ATP).[3] This general functioning principle is particularly attractive for the design of active materials made of fully artificial constituents. It was shown that a number of synthetic

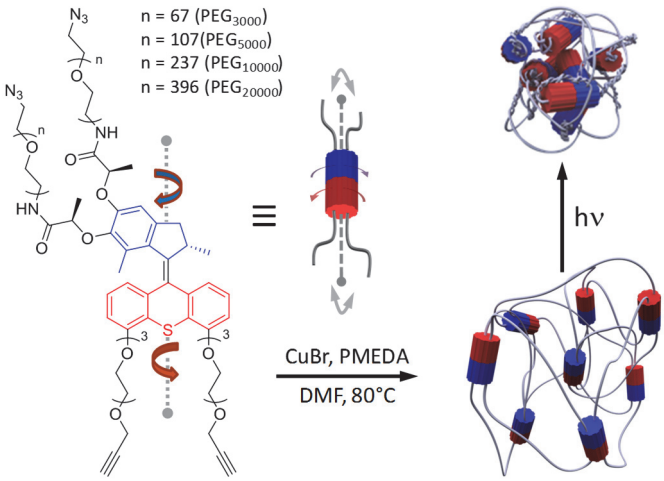

Figure 1. Schematic representation of chemical gels (bottom right) cross-linked by light-driven rotary motors (blue and red cylinders represent the branched motor units with their extended chemical structures shown on the left). By actuating the repeated unidirectional rotation of the molecular motors with UV light, the winding of the PEG chains leads to a contraction of the entire polymer network up to macroscopic scale (top right).

polymer systems that integrate artificial molecular switches (*i.e.* that function at thermodynamic equilibrium) can amplify nanoactuations across increasing length scales.[4–18] However, the integration of more complex artificial molecular motors[19–26] (*i.e.* that function out of thermodynamic equilibrium) are still very scarce although extremely attractive. Indeed, they would result in truly active synthetic materials capable of continuously and autonomously cycling workloads when fuelled by a constant energy input. A system of interest in this direction was developed recently by using Feringa's light-driven rotary motors[27–29] as reticulation nodes into (polyethylene glycol (PEG))-based chemical gels (Figure 1).[30,31] By designing cross-links with proper topologies, and upon UV light activation, it was proposed that the unidirectional rotation of the motors enforces the conformational winding of pairs of polymer chains at the nanoscale, that in turn enforce the irreversible macroscopic contraction of the material. It was

[a] *SAMS Research Group, Institut Charles Sadron, CNRS, University of Strasbourg, 23 rue du Loess, BP 84047, 67034 Strasbourg Cedex 2, France*
E-mail: giuseppone@unistra.fr
[b] *Institut Charles Sadron, CNRS, 23 rue du Loess, BP 84047, 67034 Strasbourg Cedex 2, France*
[c] *Matière et Systèmes Complexes (MSC) Laboratory, UMR CNRS 7057, Sorbonne Paris Cité, University of Paris Diderot-Paris VII, Bâtiment Condorcet, 75205 Paris Cedex 13, France*
E-mail: eric.buhler@univ-paris-diderot.fr.

Electronic Supplementary Information (ESI) available: Synthetic protocols and characterization of key compounds, synthetic protocols for the formation of gels, procedures for the rheology measurements and irradiation experiments, SANS experimental procedures and supplementary experiments. See DOI: 10.1039/x0xx00000x

also shown that, by using additional rotary molecular elements capable of unwinding the polymer chains, it becomes possible to reset the twisted polymer network to its original size.[32] Now we perform the first mechanical study of this contraction process by using a combination of rheology and small angle neutron scattering (SANS) experiments. We correlate important parameters with the potential energetic efficiency of the system, such as the critical overlap concentration of the polymers (c^*), the presence of heterogeneities in the gel, and the number of twisting strands.

Results and discussion

All experiments in the following study were performed with fully swollen gels at room temperature in toluene, and using a home-made piezorheometer at various frequencies comprised between 1 Hz and 100 Hz. As a very first observation, only the shear modulus G' was measurable. Indeed, in these systems, the loss modulus G'' was in the measurability limit (see Supporting Information (SI) section 2 for details). In addition, for all samples, G' was constant over the whole frequency range as it is usually observed for chemical polymer gels at low frequency (in the hydrodynamic regime), thus giving access to the elastic modulus of the material (Figure 2a). For all samples as well, the ratios between the G' values before and after irradiation were approximately equal to the inverse ratios of the volumes measured for the gels before and after contraction ($G'_f/G'_i \approx V_i/V_f$) (see also SI section 3 and supplementary video for the contraction under irradiation). In particular, we explored the effect of the polymer length used in the gel on the mechanical properties of the materials. To do so, four different gels were formed from motors functionalized by PEG chains with molecular weights varying between 3000 g/mol and 20000 g/mol, namely PEG_{3000}, PEG_{5000}, PEG_{10000} and PEG_{20000} (Figure 2b). For all of these gels, the initial concentration of motor when preparing the gel (*i.e.* before cross-linking by "click" Cu(I)-catalyzed Huisgen 1,3-dipolar cycloaddition) was fixed at 5 mM. This implies that every sample included the same number of motors, making the polymer length the only variable parameter. In this case, we identified a maximum of efficiency (*i.e.* a maximum variation of G' before and after irradiation) for an optimal molecular weight $M_{opt} \approx 5000$ g/mol. Then, a second set of five different gels were formed keeping M_{opt} constant, but by varying the initial concentration of motor between 4 mM and 40 mM, a concentration which is also proportional to the polymer strand concentration. The plot of these data in Figure 2c shows that the maximum efficiency of the gel contraction is obtained for an optimal concentration $c_{opt} \approx 5$ mM.

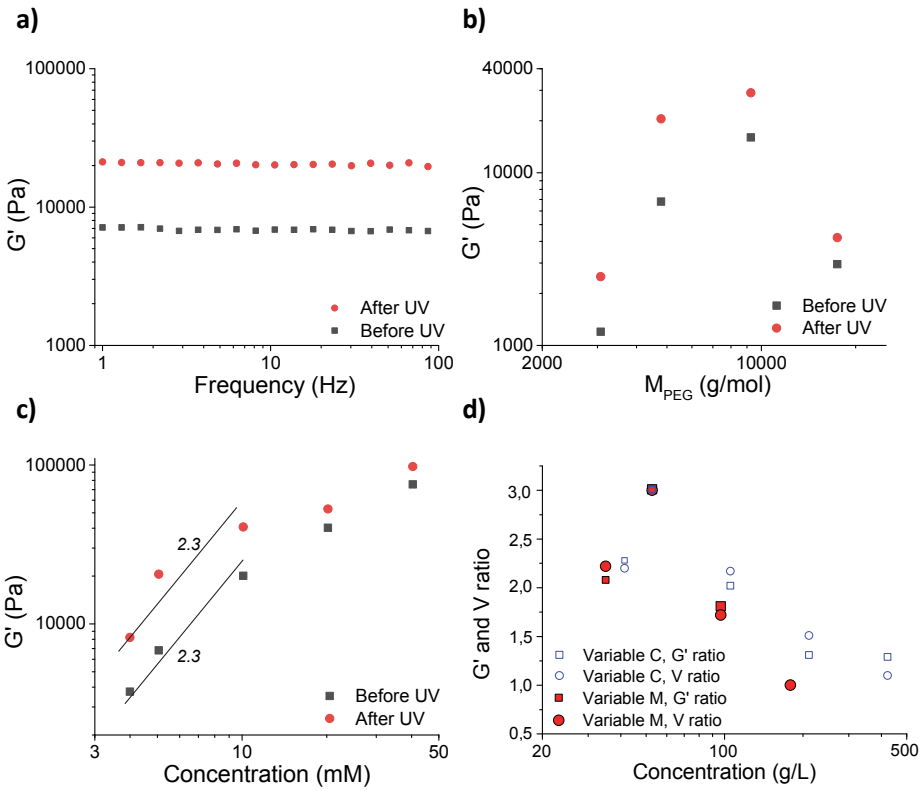

Figure 2. a) Variation of G' before and after UV irradiation, as a function of shear frequency, for a gel based on PEG_{5000} (n = 107 in Figure 1); **b)** Influence of the polymer length on the values of G' before and after UV irradiation for gels obtained from a same initial concentration of motor of 5 mM; **c)** Influence of the initial concentration of motor on the values of G' before and after UV irradiation for gels obtained from a same PEG length with a M_W of ~5000 g/mol (PEG_{5000}); below 4 mM the gels were not strong enough to be manipulated. Note that the motor concentration is proportional to the polymer strand concentration. The slope of 2.3 is simply a guide for the eye; **d)** Contraction efficiencies (*i.e.* modulus and volume ratios) of 9 different gels as a function of the mass concentration in polymer be-fore chemical cross-linking. The experimental data are combined with those used in **b)** (red) and **c)** (blue). The error bars on the measurements are smaller than the size of the data points.

To get a better insight into these experimental data, it is important to remember that the studied gels are at equilibrium and are thus fully swollen with solvent. Obukhov *et al.* predicted a scaling relationship between the elastic modulus and the polymer volume fraction in the fully swollen state, ϕ_s

$G \sim \phi_s^{3\upsilon/(3\upsilon-1)} \sim \phi_s^{2.3}$ (1)

Where υ = 0.588 in good solvent.[33,34] Note that this model and the *c** theorem predict the identical dependence of *G* on ϕ_s.[35] Data in Figure 2c shows this dependency, at least for the first part of the curve. For larger concentrations, the slope is lower suggesting that concentrated gels may present a higher number of heterogeneities which deviates the system from ideality. Interestingly the scaling law is the same for non-irradiated and irradiated gels indicating that they are both in their own equilibrium state (maximum swelling) at least for concentrations lower than 10 mM. Any gel swells until V_{eq} for which the osmotic and elastic contributions to the free energy are balanced.[33] For the non-irradiated gel, we determined experimentally an equilibrium swelling ratio $Q = V_{eq}/V_{dry}$ = 5.48×10^{-2} cm^3/0.2646×10^{-2} cm^3 = 20.7 at a concentration of 5 mM in motor and for PEG_{5000}. This is in very good agreement with the theoretical prediction in good solvent if one considers an excluded volume parameter $v \sim 0.3b^3$:

$Q = \frac{V_{eq}}{V_{dry}} = \frac{1}{\phi_s} \approx \left(\frac{v}{b^3}\right)^{0.40} N^{0.57} \phi_0^{-1/4}$ for $1/Q < \phi_0 < \phi^{**}$ (2)

Where V_{dry} is the volume of the material in the dry state (ϕ = 1), *b* is the Kuhn length, *N* = 110 the number of monomers in PEG_{5000} polymer strands, and $\phi^{**} \approx v/b^3$ the crossover concentration.

Inspection of Figure 2c also allowed us to identify the maximum contraction efficiency for a given motor concentration, c_{opt}, which is equal to 5 mM. A key parameter to understand this rheological behaviour is the number of entanglements in the samples. Chains begin to overlap when their volume fraction exceeds the overlap concentration, ϕ^*. This crossover concentration separating dilute and semi-dilute regimes, where chains interpenetrate and form a physical network, decreases with the chain length (or equivalently the degree of polymerization) with $\phi^* \sim N^{-4/5}$ in good solvent and can be estimated by measuring the size *R* of the expanded chains in dilute regime: $\phi^* \sim N/R^3$.[33] SANS performed on a dilute PEG_{5000} motor solution (*i.e.* before interconnection by "click" reaction) gives a radius of gyration of R_g = 4.3 nm (see SI, section 4) and a critical overlap concentration $c^* \sim M/(4/3\pi R_g^3 N_{Avogadro})$ = 55 g/L, which corresponds to a molar concentration of motors equal to 5.3 mM. One thus finds that, remarkably, $c^* \approx c_{opt}$. The two sets of experiment can be combined in a single graph by plotting *G'* and *V* ratios as a function of the sole mass concentration related to the degree of interpenetration of each material (Figure 2d). The maximum of the curve that corresponds to the maximum contraction efficiency ($G'_f/G'^{max}_i = V_i/V_f^{max}$ = 3) is obtained for ~*c** and reveals the major role played by this parameter.

At this point, we have revealed a general condition of preparation to reach an optimal gel contraction with any polymer chain and by simply making use of a single parameter *c**. One can postulate that below *c** the efficiency of the click reaction is reduced and the gel is not fully cross-linked, thus decreasing both its initial elastic modulus before contraction and its contraction efficiency because non-cross-linked motors cannot wind polymer chains. Above *c**, the system is denser as it includes additional physical cross-links which participate in increasing *G'* before contraction. However, these physical cross-links become detrimental to the winding of the polymer chains by the motors, and the efficiency of the contraction decreases when increasing concentration.

To refine this general picture, we complemented this study by SANS, a powerful tool to investigate the local conformation as well as the degree of aggregation of objects in the range of 1-30 nm. SANS were performed for PEG_{5000} gels at *c** (Figure 3). The SANS signal, which is the variation of the scattered intensity as a function of the scattering wave vector *q*, arises mostly from the PEG chains in the network (and less from the motor distribution). This is shown in the intermediate and high *q* regimes displaying the characteristic behaviour of excluded volume chains with a characteristic $q^{-1/\upsilon}$-q^{-1} transition, with υ = 0.588 and a Lorentzian variation associated with the correlation length that is the mesh size of the entangled network. The low *q* upturn, well observed before irradiation, is associated to heterogeneities. By refining these data one can see that: *i*) At high-*q*, the extended and contracted curves are superimposed. The q^{-1} dependence is characteristic of the rod-like behaviour of the chains for distances smaller than the persistence length, l_p, while the $q^{-1.7}$ one is typical for a polymer chain expanded in a good solvent. The crossover *q* value between these dependencies identifies the persistence length of the polymers that remains unchanged and equal to l_p = 1.1 nm. *ii*) In the mid-*q* region, the initial gel signal bends over at higher *q* values compared to the contracted one. Here, the SANS signal arises from the network itself since it follows a Lorentzian law which can be associated to the mesh size of the polymer network. For the contracted system, the excluded volume regime $q^{-1.7}$ is extended to much lower *q* values, indicating that the mesh of the network is much larger. *iii*) At low-*q*, the q^{-3} increase observed for the extended gel indicates the presence of heterogeneities larger than the scattering length scale, *i.e.* larger than 40 nm. Under contraction, the Lorentzian variation associated with the mesh size of the network extends to much lower *q* values. The signal of heterogeneities may thus arise at much lower *q* values (the onset of an upturn seems visible at ~3×10^{-3} Å^{-1}) and/or is mixed with the Lorentzian variation that does not converge to a low *q* plateau. These experiments show that upon contraction, and counterintuitively, the mesh of the network increases in size. To determine the characteristic sizes, data were fitted by using a model combining an Ornstein-Zernicke variation at mid *q* and associated to the mesh of the polymer network with a classical low *q* Guinier expression allowing an estimate of the heterogeneities (see details in the experimental section).

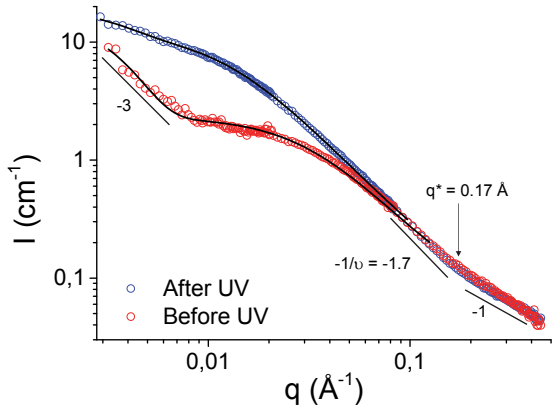

Figure 3. SANS curves before and after contraction of a PEG_{5000} gel obtained at a preparation concentration of 5 mM in motor (equal to c*). Solid lines represent the best fits of the data using the model (see SI, section 5).

Upon contraction, the mesh size grows from 5.2 ± 0.2 to 9.7 ± 0.2 nm, while the size of the heterogeneities instead remains constant around 60 ± 15 nm; however, it is difficult to have an accurate estimation of this value since its dimension is out of the available *q*-region. Formation of heterogeneities can originate from inhomogeneous distribution of polymer chains that result in partial aggregation of motors, but also from residual motors segregation before cross-linking as confirmed by SANS (see Figure S6 in SI). Formation of heterogeneities is usually inherent to gel formation and makes it difficult to estimate the density of cross-links and thus of polymer strands.[36] To determine these values, we may assume that the change of volume, which is a consequence of the rotation of the motors, is related to the amount of solvent within the gel under contraction as for classical swollen gels. This is an approximation because irradiated and non-irradiated gels have different equilibrium swellings. We thus consider that $V_0\phi_0 = V\phi = V_{dry}$, where ϕ_0 is the polymer volume fraction in the preparation state after cross-linking and ϕ the volume fraction of interest in the swollen or partly swollen state. V_0 and V are the corresponding volumes. According to the Panyukov model,[37] the elastic energy of a swollen or deformed network strand can be given by

$$F_{el} \cong kT\frac{(\lambda R_0)^2}{R_{ref}^2} \quad (3)$$

$\lambda=(V/V_0)^{1/3}=(\phi_0/\phi)^{1/3}$ is the linear deformation, $R^2=(\lambda R_0)^2$ is the mean-square end-to-end distance of network strands in the final state (*e.g.* at equilibrium or in a swollen/deswollen state), and R_{ref}^2 is the mean-square fluctuation of the end-to-end distance of the network strand that in many cases is equal to the mean-square end-to-end distance of a free chain with the same number of monomers as the strand in the same solution (here 110 PEG units for M_{opt}). The elastic modulus of the gel $G(\phi)$ in the swollen or partly swollen (deswollen) state is proportional to the chain number density, ϕ/Nb^3, times the elastic free energy per chain. In good solvent regime and for $1/Q<\phi_0<\phi^{**}$ we have:

$$G(\phi) \cong kT\frac{\phi}{Nb^3}\left(\frac{\lambda R_0}{R_{ref}}\right)^2 \cong kT\frac{\phi}{Nb^3}\left(\frac{\phi_0}{\phi}\right)^{2/3}\left(\frac{\phi}{\phi_0}\right)^{(2\upsilon-1)/(3\upsilon-1)} \quad (4)$$

With υ = 0.588 as shown by SANS. Before irradiation, the concentration of polymer is the concentration of preparation, which is equal to the crossover concentration for the optimal system: $\phi = \phi_0 = \phi^*$ with $\lambda = 1$. Using the experimental value of the modulus G' = 6800 Pa, one obtains an initial number density of effective polymer strands equal to $(\phi/Nb^3)_{initial} \cong 6800/kT \cong 1.65\times10^{24}$ strands/m^3, a value smaller than the polymer density used for the preparation of the gel and indicating that a large part of the material is within the heterogeneities. Other chains such as trapped entanglements, loops, dangling ends, and other connectivity defects are also elastically ineffective strands that do not contribute to G. When contracted $\phi_0/\phi = V/V_0 = (1.82\times10^{-2}$ cm^3/5.48×10^{-2} cm^3) = 1/3 = λ^3 and G' = 20527 Pa, one can extract a final number density $(\phi/Nb^3)_{final} \cong 8.06\times10^{24}$ strands/m^3, a value 5 times larger than the initial one and indicating that N has decreased due to the formation of new entanglements. This is a direct experimental observation at nanoscale that the motors rotation indeed twists pairs of neighbouring polymer chains leading to the formation of new entanglements which play the role of additional cross-links that increase the elastic modulus. Because the winding of the polymer chains leaves more space between the newly entangled domains, it increases the averaged mesh size of the network at the same time. Finally, this 5 times increase in the number of polymer strands during the rotation/contraction process may be related to an energy which is proportional to the number of new strands times the elastic energy per chain. It confirms that this type of motorized system can convert light energy toward elastic energy.

Conclusions

By combining rheology studies and SANS experiments, we have determined a number of important guidelines to design and potentially improve the efficiency of this first generation of motorized active gels. The most critical parameter to optimize these systems is the preparation concentration (before chemical cross-linking) which should be close to the critical overlap concentration of the polymer chains. It permits to maximize the number of active reticulation units, while limiting the number of additional inactive entanglements that break the efficiency of the motors. The second important aspect of these gels is the presence of heterogeneities which produce a number of elastically ineffective strands and preclude reaching the maximum theoretical efficiency of the material. It strongly suggests that the improvement of the gel homogeneity by chemical design, as also thoroughly discussed for more classical gels in the literature,[38,39] could be of particular interest to enhance their dynamic behaviour. Finally, this first mechanical study confirms experimentally that the macroscopic contraction of such materials is the direct result of the increase of polymer strands when winded by the rotary motors, thus relating the light energy input with the stored elastic energy. Our characterizations also reveal a particularly original and unexpected behaviour of these gels in which the microscopic mesh size of the network increases while the

entire material produces a macroscopic contraction. The efforts reported here towards a deeper understanding of these complex systems will be instrumental in reaching the general objective of implementing molecular motors in active polymer materials.

Conflicts of interest

There are no conflicts to declare.

Acknowledgements

This work was supported by the Agence Nationale pour la Recherche (INTEGRATION project, Grant number ANR-14-CE06-0021, fellowships to G.M.). We wish to thank the Laboratory of Excellence for Complex System Chemistry (LabEx CSC, fellowships to J.-R.C.-I.), the Chinese Scholarship Council (CSC, fellowship to Q.L.), and the Institut Laue Langevin (ILL, Grenoble, France) for beamtime allocation.

Notes and references

1 M. Schliwa and G. Woehlke, *Nature*, 2003, **422**, 759–765.
2 R. D. Vale and R. A. Milligan, *Science*, 2000, **288**, 88–95.
3 J. L. Krans, *Nat. Educ.*, 2010, **3**, 66–69.
4 R. S. Stoll and S. Hecht, *Angew. Chem. Int. Ed.*, 2010, **49**, 5054–5075.
5 G. Du, E. Moulin, N. Jouault, E. Buhler and N. Giuseppone, *Angew. Chem. Int. Ed.*, 2012, **51**, 12504–12508.
6 J. Chen, F. K.-C. Leung, M. C. A. Stuart, T. Kajitani, T. Fukushima, E. van der Giessen and B. L. Feringa, *Nat. Chem.*, 2018, **10**, 132–138.
7 D. J. van Dijken, J. Chen, M. C. A. Stuart, L. Hou and B. L. Feringa, *J. Am. Chem. Soc.*, 2016, **138**, 660–669.
8 Q. Lin, X. Hou and C. Ke, *Angew. Chem. Int. Ed.*, 2017, **56**, 4452–4457.
9 Y. Lin, X. Jiang, S. T. Kim, S. B. Alahakoon, X. Hou, Z. Zhang, C. M. Thompson, R. A. Smaldone and C. Ke, *J. Am. Chem. Soc.*, 2017, **139**, 7172–7175.
10 A. Goujon, G. Du, E. Moulin, G. Fuks, M. Maaloum, E. Buhler and N. Giuseppone, *Angew. Chem. Int. Ed.*, 2016, **55**, 703–707.
11 A. Goujon, G. Mariani, T. Lang, E. Moulin, M. Rawiso, E. Buhler and N. Giuseppone, *J. Am. Chem. Soc.*, 2017, **139**, 4923–4928.
12 A. Goujon, T. Lang, G. Mariani, E. Moulin, G. Fuks, J. Raya, E. Buhler and N. Giuseppone, *J. Am. Chem. Soc.*, 2017, **139**, 14825–14828.
13 L. Gao, Z. Zhang, B. Zheng and F. Huang, *Polym. Chem.*, 2014, **5**, 5734–5739.
14 A. Wolf, E. Moulin, J. J. Cid Martín, A. Goujon, G. Du, E. Busseron, G. Fuks, N. Giuseppone, *Chem. Commun.,* 2015, **51**, 4212-4215.
15 K. Iwaso, Y. Takashima and A. Harada, *Nat. Chem.*, 2016, **8**, 625–632.
16 M. Nakahata, Y. Takashima, H. Yamaguchi and A. Harada, *Nat. Commun.*, 2011, **2**, 511.
17 Y. Yu, M. Nakano and T. Ikeda, *Nature*, 2003, **425**, 145–145.
18 Y. Yu, T. Maeda, J. Mamiya and T. Ikeda, *Angew. Chem. Int. Ed.*, 2007, **46**, 881–883.
19 T. R. Kelly, H. De Silva and R. A. Silva, *Nature*, 1999, **401**, 150–152.
20 J. Wang and B. L. Feringa, *Science*, 2011, **331**, 1429–1432.
21 L. Greb and J.-M. Lehn, *J. Am. Chem. Soc.*, 2014, **136**, 13114–13117.
22 G. Ragazzon, M. Baroncini, S. Silvi, M. Venturi and A. Credi, *Nat. Nanotech.*, 2015, **10**, 70–75.
23 S. Kassem, A. T. L. Lee, D. A. Leigh, V. Marcos, L. I. Palmer and S. Pisano, *Nature*, 2017, **549**, 374–378.
24 C. Cheng, P. R. McGonigal, S. T. Schneebeli, H. Li, N. A. Vermeulen, C. Ke and J. F. Stoddart, *Nat. Nanotech.*, 2015, **10**, 547–553.
25 R. D. Astumian, *Science*, 1997, **276**, 917–922.
26 W. R. Browne and B. L. Feringa, *Nat. Nanotech.*, 2006, **1**, 25–35.
27 N. Koumura, R. W. J. Zijlstra, R. A. van Delden, N. Harada and B. L. Feringa, *Nature*, 1999, **401**, 152–155.
28 B. L. Feringa, *Angew. Chem. Int. Ed.*, 2017, **56**, 11060–11078.
29 R. Eelkema, M. M. Pollard, J. Vicario, N. Katsonis, B. S. Ramon, C. W. M. Bastiaansen, D. J. Broer and B. L. Feringa, *Nature*, 2006, **440**, 163.
30 Q. Li, G. Fuks, E. Moulin, M. Maaloum, M. Rawiso, I. Kulic, J. T. Foy and N. Giuseppone, *Nat. Nanotech.*, 2015, **10**, 161–165.
31 Q. Li, J. T. Foy, J.-R. Colard-Itté, A. Goujon, D. Dattler, G. Fuks, E. Moulin and N. Giuseppone, *Tetrahedron*, 2017, **73**, 4874–4882.
32 J. T. Foy, Q. Li, A. Goujon, J.-R. Colard-Itté, G. Fuks, E. Moulin, O. Schiffmann, D. Dattler, D. P. Funeriu and N. Giuseppone, *Nat. Nanotech.*, 2017, **12**, 540–545.
33 M. Rubinstein and R. H. Colby, *Polymer physics*, Oxford University Press, Oxford, New York, 2003.
34 S. P. Obukhov, M. Rubinstein and R. H. Colby, *Macromolecules*, 1994, **27**, 3191–3198.
35 P. G. de Gennes, *Scaling Concepts in Polymer Physics*, Cornell University Press, Ithaca, 1979.
36 T. Katashima, U. Chung and T. Sakai, *Macromol. Symp.*, 2015, **358**, 128–139.
37 S. V. Panyukov, *Sov. Phys. JETP*, 1990, **71**, 372–379.
38 M. Shibayama, *Macromol. Symp.*, 2017, **372**, 7–13.
39 T. Sakai, T. Matsunaga, Y. Yamamoto, C. Ito, R. Yoshida, S. Suzuki, N. Sasaki, M. Shibayama and U. Chung, *Macromolecules*, 2008, **41**, 5379–5384.